Food Chemistry: X 23 (2024) 101706

Contents lists available at ScienceDirect

Food Chemistry: X

journal homepage: www.sciencedirect.com/journal/food-chemistry-x

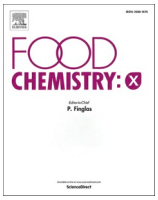

Structural, antioxidant activity, and stability studies of jellyfish collagen peptide–calcium chelates

Jiajia Gao [1], Chong Ning [1], Mingxia Wang, Mingming Wei, Yifei Ren, Weixuan Li [*]

College of Light Industry, Liaoning University, Shenyang 110036, PR China

ARTICLE INFO

Keywords:
Jellyfish (*Rhopilema esculentum Kishinouye*)
collagen peptide
Peptide-calcium chelate
Structural characterization
Antioxidant activity
Stability

ABSTRACT

The aim of this study was to prepare and characterize jellyfish collagen peptide (JCP)–calcium chelates (JCP-Ca) using peptides with different molecular weights. Further analysis revealed that the low-molecular-weight jellyfish collagen peptide (JCP1) had a higher chelation rate. Structural characterization showed that functional groups such as N—H, C═O, and -COO were involved in the formation of JCP-Ca, which shifted towards a more ordered and regular structure, and smaller-molecular-weight peptides were more likely to form a denser structure. In addition, JCPs chelated with calcium ions showed excellent antioxidant capacity. JCP-Ca showed good stability in heat-treated and gastrointestinal environments, whereas the antioxidant activity was significantly reduced under highly acidic conditions. The present study addresses the knowledge gap regarding the physicochemical properties of JCP-Ca and establishes a solid research foundation for its associated products.

1. Introduction

The jellyfish (*Rhopilema esculentum* Kishinouye), a species of the Rhizostomatidae family, is widely distributed in the coastal waters of China and is abundant in Liaoning, Zhejiang, and Jiangsu. Jellyfish is rich in nutritional value and contains high-quality proteins, polyunsaturated fatty acids, phospholipids, triglycerides, iodine, iron, zinc, calcium, and other minerals (Yu et al., 2014). In addition, Jellyfish has therapeutic effects, such as removing heat, detoxification, resolving and softening phlegm, lowering blood pressure, and reducing swelling. Jellyfish are also used for the treatment of bronchitis, gastric ulcers, and asthma. Jellyfish are rich in collagen and free of crude fat. Jellyfish collagen offers numerous positive benefits, including antioxidant, anti-inflammatory, immunomodulatory, and hypolipidemic effects (Lv, Zhang, Song, Chen, & Wang, 2022). Very small bioactive peptides with interesting biological activities are produced via enzymatic hydrolysis. Bioactive peptides generated from collagen have immunomodulatory properties owing to their unique amino acid composition (Fan, Zhuang, & Li, 2013), as well as angiotensin-converting enzyme (ACE)-inhibitory (Hu et al., 2023), antimicrobial, wound-healing, and antioxidant properties(Zhang et al., 2022).

The presence of metal ions is essential for the survival of living organisms. When collagen or collagen peptides are chelated with metal elements, the properties of the metal usually confer better structural stability and unique physicochemical properties to the chelated compounds. Moreover, biophilic metals exhibit biocompatibility with chelated collagen and can effectively prevent biological rejection (Wu et al., 2022). The relative molecular mass of collagen peptides is low and when chelated with calcium, chromium, iron, copper, zinc, and other essential metal elements, their dissolution and absorption effects are more apparent, which is conducive to the production of food and healthcare products for humans, such as calcium and iron supplements (Ge et al., 2023). Examples of this include iron-peptides chelating nanoliposomes when iron supplements are provided to rats, demonstrating that the mildly adverse effects of nanoliposome-encapsulated iron-peptides are outweighed by the considerable therapeutic effect of iron supplementation (Chen et al., 2023). Wang et al. studied a casein peptide–iron chelate, with their findings suggesting the possibility of using it as a dietary addition to enhance iron digestion (Wang et al., 2022). After the binding of peptides prepared from Antarctic krill to zinc

Abbreviations: JCP, jellyfish collagen peptides; JCP-Ca, jellyfish collagen peptide-calcium chelate; FT-IR, Fourier-transform infrared; CD, circular dichroism; UV, ultraviolet; 3D, three-dimensional; DPPH, 1,1- diphenyl-2-picrylhydrazyl; ABTS, 2,2-azino-bis (3-ethylbenzothiazoline-6-sulfonic acid) diammonium salt.

* Corresponding author at: College of Light Industry, Liaoning University, No.66 Chongshan Middle Road, Huanggu District, Shenyang, Liaoning Province, PR China.

E-mail address: liweixuan@lnu.edu.cn (W. Li).

[1] Jiajia Gao and Chong Ning have contributed equally to this work

https://doi.org/10.1016/j.fochx.2024.101706
Received 20 March 2024; Received in revised form 9 July 2024; Accepted 26 July 2024
Available online 31 July 2024

ions, the resulting cation could effectively encourage human zinc absorption (Sun et al., 2021).

Calcium is an essential inorganic element that accounts for 1.5–2.2% of the total weight of the body (Peng, Hou, Zhang, & Li, 2017). It has a regulatory function in endocellular metabolism and promotes bone development and nerve transmission. Many illnesses, including rickets, hypertension, and osteoporosis, are caused by calcium deficiency, which is a major public health concern worldwide. Chronic calcium deficiency in children leads to slow growth and rickets, whereas calcium deficiency in the elderly predisposes them to diseases such as osteoporosis (Xiang et al., 2022), which can be ameliorated by increasing dietary calcium intake and absorption. Importantly, the body can only restore calcium stores in the bones through dietary consumption (Sun et al., 2020). Therefore, maintaining good bone health requires sufficient calcium provided by the diet.

Several types of calcium supplements are available, including inorganic, organic, and amino acid-derived forms. However, their use is associated with several disadvantages, including the accumulation of insoluble calcium salts in the human gastrointestinal tract and low absorption (Wu et al., 2019). Peptide-chelated calcium is more soluble and bioavailable and causes less irritation to the human digestive system than other calcium supplements. Therefore, it is now generally acknowledged that calcium–peptide chelates could be superior calcium supplements that could substantially enhance the absorption of calcium by the gastrointestinal tract (Zhang & Liu, 2022). Numerous peptides that can bind calcium ions have been isolated from plants and animals and studied. These include the low-molecular-weight collagen peptide that is extracted from the skin of white carp, which can bind calcium ions (Yang et al., 2021), the binding of low-molecular-weight collagen peptides from marlin bone to calcium ions (Zhong et al., 2023), and Manchurian walnut meal integrated with calcium ions (Fang, Ruan, Hao, Regenstein, & Wang, 2020). These results demonstrate the feasibility of preparing peptide–calcium chelates and their potential as calcium supplements.

However, few researchers have focused on extracting proteins and bioactive peptides from jellyfish. There were few reports on the use of jellyfish hydrolysate as a source of calcium-binding peptides. In the current study, jellyfish collagen peptides (JCPs) of different molecular weights were prepared and peptide–calcium chelates (JCP-Ca) were generated. Ultraviolet (UV) spectroscopy, fluorescence spectrophotometry, scanning electron microscopy, three-dimensional fluorescence, Fourier-transform infrared (FT-IR) spectroscopy, and circular dichroism (CD) spectrophotometry were used to assess the structural characteristics of these materials. In addition, the antioxidant activity of the peptide–calcium chelates, as well as their stability, was evaluated and determined by simulating gastrointestinal digestion *in vitro* under different conditions. The results of this study encourage the utilization of jellyfish resources and provide a solid scientific basis for the development of novel dietary supplements containing calcium.

2. Materials and methods

2.1. Materials

Jellyfish were purchased from the Tawan Seafood Market, Shenyang, and flavored protease (20,000 U/g), pepsin (1:3000), and trypsin (1:250) were purchased from Shenyang Laboratory Science and Trading Co., Ltd. (Liaoning, China). All chemicals were of analytical grade.

2.2. Preparation of JCPs of different molecular weights

Fresh jellyfish were cleaned and soaked in acetone for 24 h and then in disodium hydrogen phosphate for 24 h, washed until they were odorless, and sliced using scissors into homogenous pieces of 2–3 cm. A phosphate buffer rinse at pH 7.4 was added to 0.5 g/mL of the homogenate and a flavor protease, was added at 4.0% of the substrate mass; the enzyme was digested for 4 h in a water bath at 44 °C. Enzyme digestion was allowed to continue for 4 h under these conditions, with Tris-HCl buffer (pH 8.3) added at a ratio of 1:2 to the substrate liquid; 3.0% trypsin, based on the substrate mass, also added. Following the reaction, the enzyme was inactivated by heating for 10 min in a boiling water bath. The mixture was then centrifuged for 10 min at 25 °C and 10,000 ×*g*. The supernatant was collected at the end of centrifugation, and omega membranes with different molecular weights were used to intercept the JCPs. JCP1 (jellyfish collagen peptide component 1, <1 kDa), JCP2 (jellyfish collagen peptide component 2, 1–3 kDa), JCP3 (jellyfish collagen peptide component 3, 3–10 kDa), and JCP4 (jellyfish collagen peptide component 4, >10 kDa) were obtained, and the samples were freeze-dried under a vacuum at −80 °C for 48 h and stored in a refrigerator at 4 °C for later use.

2.3. Sodium dodecyl sulphate–polyacrylamide gel electrophoresis (SDS-PAGE)

A 5 mg/L sample solution was mixed with the sample buffer containing 10% glycerol, 3% SDS, 0.05% bromophenol blue, and 5% -mercaptoethanol in equal proportions. This was heated at 100 °C for 5 min. A separation gel with a concentration of 12% and a concentration gel 5% were prepared and Operated at different voltages. Finally, the finished gel was dyed for 30 min using 0.02% Coomassie brilliant blue R-250 solution and decolorized using a decolorizing solution (methanol: acetic acid: ultrapure water = 1:2:17) until the gel was colorless (Yang et al., 2024).

2.4. Amino acid composition analysis

An amount of 100 mg of the sample was weighed in a hydrolysis tube, 10 mL of 6 mol/L HCl was added and the sample was allowed to dissolve before filling with nitrogen for 3 min and hydrolysing at 110 °C for 24 h. After cooling, water was added to 50 mL. An amount of 5 mL of the sample was placed in an evaporating dish to evaporate. During this time, the sample was rinsed and concentrated with distilled water three times, and then put through a 0.22-μm filter membrane. The sample was analyzed on an automatic amino acid analyzer (L-8800, Hitachi, Ltd., Japan).

2.5. Preparation of JCP-ca

The four lyophilized components of JCP were dissolved in 30 mg/mL of distilled water and 1 M sodium hydroxide or 1 M hydrochloric acid was added to adjust the pH to 9. Calcium chloride (jellyfish collagen peptide: anhydrous calcium chloride) was added at a mass ratio of 3:1 and uniformly mixed. The peptide–calcium chelates were obtained by adding anhydrous ethanol, at three times the bulk volume, after 3 h of alcohol precipitation with constant-temperature oscillations using a magnetic stirrer with a reaction temperature of 50 °C for 30 min. The precipitates were centrifuged at 10,000 ×*g* for 10 min, and the precipitate was collected and freeze-dried for 48 h to obtain the peptide–calcium chelate. For the determination of the calcium chelation rate, the ethylenediaminetetraacetic acid (EDTA) titration method was used (Zhong et al., 2023):

$$C(\%) = \frac{V_1}{V_2} \times 100 \quad (1)$$

where V_1 denotes the bulk EDTA used to titrate a specific chelated ion, and V_2 is the bulk EDTA used to titrate the total concentration of the specific ion.

2.6. FT-IR spectroscopy

The lyophilized sample (5 mg) was mixed with dried potassium

bromide at 1:100, pressed into a film, and scanned with the following parameters: wave number, 400–4000 cm^{-1}; scanning, 32 times; and resolution, 4 cm^{-1}.

2.7. CD spectra

For this, 3 mg of the lyophilized sample was taken and dissolved in a 0.15 mg/mL solution with distilled water. Spectral scanning was performed using a circular dichroic spectrometer with a scanning range of 190–250 nm at a speed of 100 nm/min and intervals of 0.5 nm, and the blank was corrected using distilled water.

2.8. UV spectra

Collagen peptides and peptide–calcium chelates were prepared in distilled water to a mass concentration of 2 mg/mL and scanned at a wavelength range of 200–400 nm using a UV spectrophotometer at 2 mm/s.

2.9. Fluorescence spectroscopy

Deionized water was used to dissolve 5 mg of the lyophilized sample to 1 mg/mL, and this was scanned and analyzed using a fluorescence spectrophotometer with a 1 cm-wide quartz cuvette, an excitation wavelength of 280 nm, an emission wavelength of 300–400 nm, a slit of 10 nm, a speed of 120 nm/min, and a voltage of 700 V. The sample was then analyzed using a fluorescence spectrophotometer with a 1 cm-wide quartz cuvette.

2.10. Three-dimensional (3D) fluorescence spectral analysis

When the excitation wavelength range was 200–350 nm and the emission wavelength range was 220–480 nm (both of which were increased with increments of 5 nm), the fluorescence signals were collected to obtain the excitation–emission matrix fluorescence spectra, i.e., the 3D fluorescence spectra.

2.11. Scanning electron microscopy (SEM)

Energy-dispersive spectrometry-equipped scanning electron microscopes operating at an accelerating voltage of 5 kV were used to acquire scanning electron images to analyze the microstructures of the various JCP-Ca components.

2.12. Determination of antioxidant capacity

2.12.1. Fe^{3+}-reducing power

The lyophilized samples were weighed and 5 mL solutions with a concentration gradient of 1, 2, 3, 4, and 5 mg/mL were prepared in phosphate buffer (pH = 6.6). Separately, 1 mL of the sample solution was removed to a test tube and 1 mL of 1% potassium ferricyanide solution was added to each test tube. The reaction was allowed to proceed for 20 min at 50 °C in a water bath and 2 mL of 10% trichloroacetic acid was then added to terminate the reaction. An amount of 1.2 mL of 0.1% ferric chloride was added, and the sample was left at 25 °C for 30 min. The concentration was taken as the horizontal coordinate, and the absorbance was taken as the vertical coordinate to construct the activity curve.

2.12.2. 1,1-Diphenyl-2-picrylhydrazyl (DPPH) radical-scavenging activity

DPPH radical-scavenging activity was determined using a slightly modified method of Wali et al. (2019). The lyophilized samples were diluted with distilled water to generate 5 mL solutions with a concentration gradient of 1, 2, 3, 4, and 5 mg/mL. Two milliliters of each sample were then transferred into test tubes, and each test tube was then filled with 2 mL of the DPPH ethanol solution. The samples were then incubated for 30 min, and the absorption intensity was measured at 517 nm. The following calculation was used:

$$\text{Clearance rate}\ (\%) = \left(1 - \frac{A_1 - A_2}{A_3}\right) \times 100 \quad (2)$$

where A_1 is the absorbance of the sample at 517 nm, A_2 is the absorbance of anhydrous ethanol instead of DPPH at 517 nm, and A_3 is the absorbance of the blank control at 517 nm.

2.12.3. 2,2-Azino-bis (3-ethylbenzothiazoline-6-sulfonic acid) diammonium salt (ABTS) radical-scavenging activity

ABTS radical-scavenging activity was determined using a slightly modified method of Wang et al. (2021). First, the ABTS stock solution was prepared: 7 mmol/L ABTS solution was combined in equal proportions with 2.45 mmol/L potassium persulfate solution and incubated for 15 h in the dark. The reserve solution was appropriately diluted using anhydrous ethanol such that the absorbance of the diluted solution at 734 nm was 0.7 ± 0.02 for the ABTS working solution.

Following lyophilization, 2 mL solutions comprising a concentration gradient of 1, 2, 3, 4, and 5 mg/mL were prepared using distilled water, and 0.4 mL of each sample was put into a test tube. The samples were then incubated at 37 °C for 10 min after adding 3.6 mL of ABTS working solution, after which the absorption value at 734 nm (A_2) was measured. The following calculation was used:

$$\text{ABTS radical} - \text{scavenging ability}\ (\%) = \left(1 - \frac{A_2 - A_0}{A_1}\right) \times 100 \quad (3)$$

where A_0 is the absorbance of distilled water and ethanol at 734 nm, A_1 is the absorbance of distilled water and ABTS working solution at 734 nm, and A_2 is the absorbance of the sample and ABTS working solution at 734 nm.

2.12.4. Hydroxyl radical (·OH)-scavenging activity

The lyophilized samples were used to make 1, 2, 3, 4, and 5 mg/mL solutions, generated using a 9 mmol/L salicylic acid–ethanol solution, 9 mmol/L $FeSO_4$ solution, and 10 mmol/L H_2O_2 solution in the dark. After 1 mL of the sample solution was placed in a test tube, 1 mL of a salicylic acid–ethanol solution, 1 mL of a $FeSO_4$ solution, and 1 mL of an H_2O_2 solution were added, and the sample was mixed well; the absorbance was measured at 510 nm for 15 min at 37 °C in a water bath. The hydroxyl radical-scavenging ability of each sample was calculated as:

$$\text{Hydroxy radical} - \text{scavenging activity}\ (\%) = \left(1 - \frac{A_1 - A_2}{A_0}\right) \times 100 \quad (4)$$

where A_0 is the absorbance of the control group (i.e., distilled water instead of samples), A_1 is the absorbance of the sample group, and A_2 is absorbance of the blank group (i.e., distilled water instead of H_2O_2 solution).

2.13. Stability studies

2.13.1. Temperature and pH

The JCP-Ca components were dissolved in distilled water to obtain a hydrolysate concentration of 5 mg/mL. After adjusting the test solutions to pH values of 2, 4, 6, 8, and 10 using 1 M HCl and 1 M NaOH, they were incubated for 1 h at 37 °C in a water bath. The hydroxyl radical-scavenging capacities were determined after cooling the JCP-Ca sample to 25 °C.

The JCP-Ca components were then dissolved in distilled water to obtain a hydrolysate concentration of 5 mg/mL. The hydrolysates were placed in a water bath at 50, 60, 70, 80, and 90 °C for 1 h. Following the holding period, the samples were cooled to room temperature and used to determine the rate at which radicals were scavenged by hydroxyl.

2.13.2. Simulated digestion in vitro

The JCP-Ca components were dissolved in distilled water to obtain a hydrolysate concentration of 5 mg/mL. The pH of the sample solution was adjusted to 2 using 1 M HCl and 1 M NaOH. Subsequently, 4% pepsin was added to the solution, and digestion was performed at 37 °C for 1 h. The pH of the gastric juice was adjusted to 7, and 4% trypsin was added. The mixture was digested at 37 °C for 2 h. At the end of the digestion process, intestinal digests were boiled immediately in a water bath for 10 min. After cooling to room temperature, hydroxyl radical-scavenging activities were determined separately. Trypsin and pepsin were not added to the control group under the same conditions.

2.14. Statistical analysis

Tests were conducted in triplicate, and the data are expressed as the mean ± standard deviation. Data were statistically analyzed using SPSS software (version 22.0; SPSS Inc., Chicago, IL, USA). Statistical differences between the samples were determined using Duncan's multiple range test, with $p < 0.05$ considered significant.

3. Results and discussion

3.1. Preparation of JCP and JCP-ca

3.1.1. SDS-page

The SDS-PAGE spectrum of jellyfish collagen peptides was characterized using SDS-PAGE electrophoresis, as shown in Fig. 1A. The molecular weights were located between 5 and 14.4 kDa, confirming that the enzymatic digest of jellyfish collagen was a collagen peptide, in which molecular masses are concentrated at 14.4 and 5.8 kDa. The electropherogram of the jellyfish collagen peptide in Fig. 1A shows two high-intensity bands at 14.4 and 22 kDa and a low-intensity band at 5 kDa. In summary, two enzymatic digests yielded a small molecule peptide fraction below 5.8 kDa.

3.1.2. Amino acid composition analysis

Amino acids are the basic substances of proteins, and the nutritional value of proteins depends largely on the amino acid composition. The amino acid composition of jellyfish collagen peptides and their different molecular weight jellyfish collagen peptides are shown in Table 1. Amino acid content increased with increasing molecular weight, which concurs with the findings of Zamorano-Apodaca et al. (2020). The most abundant amino acids detected in all the different peptide fractions were Asp, Glu, Gly, Ala, Leu, Arg, and Pro, which are considered to be the major binding sites for calcium (Lin, Cai, Wu, Lin, & Wang, 2020); these amino acids were also abundant in the unseparated fractions of jellyfish collagen peptides. Zhong et al. (2023) studied the amino acids of tuna collagen hydrolysates and found them to be abundant in Glu, Asp, Gly, and Pro, confirming the characterization of collagen peptides frequently present as mineral-binding peptides. Acidic amino acids have been recognized as essential amino acids and due to the presence of free carboxyl groups, they may promote the calcium chelating ability of proteins and peptides (Huang et al., 2021).

3.1.3. Determination of chelation rate

It is well known that the peptide molecular weight affects its capacity to chelate metal; hence, four peptide fractions with varying molecular weight components (JCP1–4) were assessed using EDTA to determine the rate at which calcium was chelated and calcium content was determined. The rate of chelation with each fraction is shown in Fig. 1B. From the figure, under the same conditions, the isolated fractions of JCPs had good Ca^{2+}-chelating ability and the chelation rate was >59%.

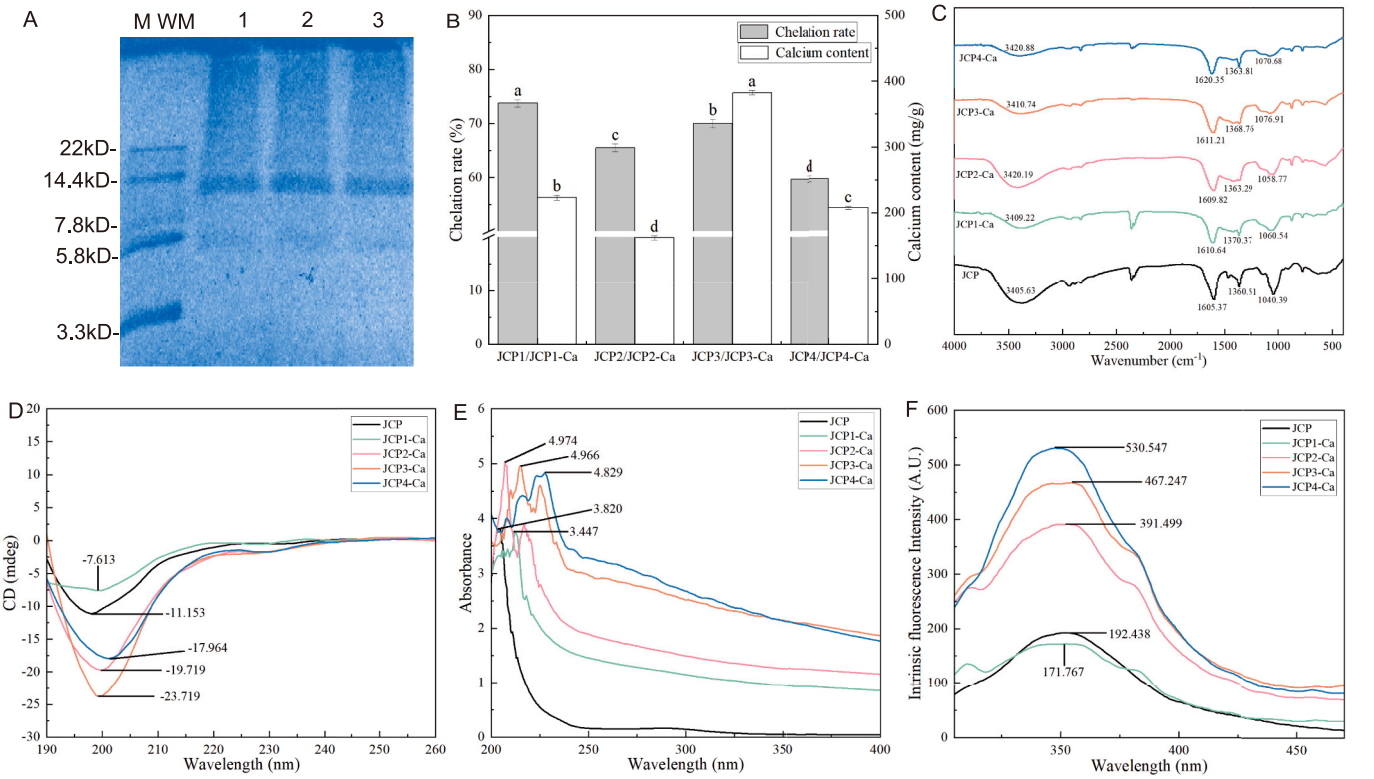

Fig. 1. Chelation rate and structural characterization of jellyfish collagen peptide (JCP) and JCP–calcium chelates (JCP-Ca). (A) The sodium dodecyl sulphate–polyacrylamide gel electrophoresis profiles of jellyfish collagen peptides. MWM: molecular weight marker in kDa, 1–3: jellyfish collagen peptides; (B) Chelation rate of JCP components of different molecular weights forming chelates with calcium and calcium content of chelates; (C) Fourier-transform infrared (FT-IR) spectroscopy data; (D) circular dichroism (CD) data; (E) ultraviolet (UV) spectra; (F) fluorescence spectra. The data are presented as mean values (mean ± SD, $n = 3$); different letters denote a statistically significant difference ($p < 0.05$).

Table 1
Amino acid contents of jellyfish collagen peptide and different molecular weights jellyfish collagen peptide.

AA	JCP (mg/g)	JCP1 (mg/g)	JCP2 (mg/g)	JCP3 (mg/g)	JCP4 (mg/g)
Asp	22.37 ± 2.07^{b}	5.33 ± 2.82^{d}	6.75 ± 1.13^{d}	17.50 ± 0.26^{c}	31.50 ± 1.14^{a}
Thr	10.38 ± 1.00^{b}	3.75 ± 0.37^{d}	3.17 ± 0.75^{d}	7.53 ± 0.53^{c}	13.88 ± 0.56^{a}
Ser	8.98 ± 0.82^{b}	3.60 ± 0.53^{d}	3.38 ± 0.70^{d}	7.53 ± 0.49^{c}	10.52 ± 0.86^{a}
Glu	23.46 ± 2.44^{b}	8.71 ± 0.34^{c}	7.09 ± 0.55^{c}	23.28 ± 0.86^{b}	29.14 ± 0.98^{a}
Gly	32.07 ± 1.68^{a}	13.46 ± 1.01^{c}	13.75 ± 0.10^{c}	30.99 ± 0.26^{a}	25.38 ± 0.91^{b}
Ala	17.50 ± 1.86^{b}	7.38 ± 2.19^{c}	5.81 ± 0.63^{c}	15.08 ± 0.68^{b}	20.67 ± 1.27^{a}
Val	11.57 ± 1.86^{b}	3.69 ± 0.45^{d}	2.91 ± 0.41^{d}	7.83 ± 0.30^{c}	14.65 ± 1.08^{a}
Met	4.33 ± 1.22^{b}	0.40 ± 0.21^{c}	0.84 ± 0.30^{c}	3.01 ± 0.57^{b}	6.78 ± 0.67^{a}
Ile	11.13 ± 2.01^{b}	3.60 ± 0.34^{d}	2.77 ± 0.31^{d}	8.65 ± 0.75^{c}	16.54 ± 1.36^{a}
Leu	14.17 ± 1.45^{b}	6.34 ± 0.57^{d}	4.67 ± 0.30^{e}	12.04 ± 0.49^{c}	22.32 ± 0.65^{a}
Tyr	3.80 ± 0.87^{b}	1.80 ± 0.27^{c}	1.25 ± 0.02^{c}	3.33 ± 0.53^{b}	6.98 ± 0.65^{a}
Phe	5.48 ± 0.52^{b}	1.71 ± 0.43^{d}	1.52 ± 0.32^{d}	4.00 ± 0.60^{c}	9.12 ± 0.13^{a}
Lys	12.17 ± 1.01^{b}	6.28 ± 0.27^{c}	6.15 ± 0.77^{c}	11.49 ± 0.59^{b}	17.61 ± 0.58^{a}
His	1.80 ± 0.60^{b}	0.85 ± 0.26^{b}	0.80 ± 0.46^{b}	1.28 ± 0.46^{b}	3.28 ± 0.87^{a}
Arg	21.97 ± 1.61^{c}	11.48 ± 1.40^{d}	11.82 ± 0.30^{d}	24.06 ± 0.49^{b}	29.23 ± 0.73^{a}
pro	21.62 ± 1.82^{b}	6.58 ± 0.70^{c}	6.22 ± 0.68^{c}	19.91 ± 0.86^{b}	32.38 ± 1.18^{a}

Asp: Aspartic acid; Thr: Threonine; Ser: Serine; Glu: Glutamic acid; Gly: Glycine; Ala: Alanine; Val: Valine; Met: Methionine; Ile: Isoleucine; Leu: Leucine; Tyr: Tyrosine; Phe: Phenylalanine; Lys: Lysine; His: Histidine; His: Histidine; Arg: Arginine; Pro: Proline.
Results were expressed as the mean ± standard deviation (n = 3). Different letters in the same row correspond to a significant difference at $P < 0.05$.

JCP1, with a molecular weight of <1 kDa, had the highest Ca^{2+}-chelation rate of 73.73 ± 0.67%, and JCP4, with a molecular weight of approximately >10 kDa, had the lowest Ca^{2+}-chelation rate of 59.63 ± 0.57%. There were significant differences in these chelation rates among the four fractions ($p < 0.05$). This could have been caused by variations in the quantity and type of amino acids in the various peptide compositions following ultrafiltration, with the JCP1 peptide having more groups capable of binding to Ca^{2+}. These outcomes could also be attributed to variations in the number of calcium-binding sites (Li, Bu, Chen, & Li, 2020). This concurs with the results of previous studies, in which peptides with molecular weights of <2 kDa showed a higher calcium-chelating capacity (Choi, Lee, Chun, & Song, 2012). In addition, Huang, Ren, and Jiang (2010) isolated and purified three peptide fragments with different molecular weights from shrimp processing by-products; here, the <1 kDa peptide component was better at chelating calcium than the >5 kDa peptide fragment. Moreover, Li et al. (2020) investigated the rate of zinc chelation with peanut peptides of different molecular weights and found the highest rate of zinc chelation was obtained using PPF3 (MW <3 kDa). Through the determination of calcium content, JCP1-Ca and JCP3-Ca (223.47 and 382.93 mg/g) were found to have higher calcium content, which was higher than the results of Huang et al. (2021). From these results, it can be concluded that a lower molecular weight results in easier calcium ion binding and good calcium chelation ability, which is a potential resource for chelating calcium preparation.

3.2. FT-IR spectroscopy

FT-IR spectroscopy can effectively distinguish the spectral differences between two substances, and the functional group region (400–4000 cm^{-1}) in the spectral map is usually used to identify the types of and changes in functional groups in the substance to be measured. The coordination process between the metallic ions and the molecules of organic groups can be reflected by changes in the peak absorbance of the carboxyl and amino groups in the electromagnetic spectrum. As shown in the Fig. 1C, the absorption peak of the collagen peptide at 3405.63 cm^{-1} is caused by the N—H stretching vibration, and after chelation, the four fractions of JCP-Ca are red-shifted to higher frequencies at 3409.22, 3420.19, 3410.74, and 3420.99 cm^{-1}, respectively. This indicates that the density of the electron cloud in the peptide of –NH becomes stronger due to the induction effect or dipole field effect, implying that $–NH_2$ could undergo a chelation reaction with Ca^{2+} to form an ammonium salt. The amide I bands, which mostly originate from the vibratory stretching of C═O, are the typical peaks of absorption in the range of 1700–1600 cm^{-1} in the signature region of the infrared spectrum of the peptide (Huang et al., 2021). The JCP absorption peak was at 1605.37 cm^{-1}, and all four fractions of JCP-Ca were slightly changed after chelation, whereas that of JCP4-Ca moved to 1620.35 cm^{-1}. The absorption peak wave number of -COO- shifted from 1360.51 cm^{-1} to a higher frequency of 1370.37 cm^{-1}, suggesting that -COO- might be bound to calcium and transformed to -COO-Ca, which could result from the calcium ion receiving free, non-bonded electrons from the carbonyl oxygen. After chelation occurred, the peak at 1040.39 cm^{-1} increased to 1076.91 cm^{-1}, suggesting that the C—O bond might be involved in chelation and the formation of a new ligand bond with calcium (Wang et al., 2017). Li et al. (2020) discovered that in a coordinated peanut peptide, the PPF3 absorption at 1029.80 cm^{-1} moved to 1110.80 cm^{-1}, suggesting the presence of -C═O oscillations or -CNC- telescoping vibrations. Moreover, the strength of the chelated substances was reduced, which could have been caused by variations in the number of carboxylic acid residues in the side chains of the polypeptide chains in the exposed groups. In addition, the absorption peaks in the low-frequency 500–800 cm^{-1} region showed substantial variations, with several peaks appearing when calcium was bound, suggesting that calcium ions were bound to collagen polypeptides mainly through interactions with carboxylate oxygen and amino nitrogen atoms in the peptide chain, similar to that observed with the hydrolysis product from Pacific cod bone (Peng et al., 2017). The results show that N—H, C═O, and –COO in JCP participate in the chelation reaction with calcium ions, which changes its original structure, and that chelation causes the peak intensity of each component of JCP-Ca to decrease.

3.3. CD analysis

Currently the most popular technique for determining the secondary structure of a protein, CD spectroscopy is a quick, easy, and more precise way to examine the conformation of proteins in solution. The CD spectra of proteins or peptides are divided into the far-UV region (190–250 nm) and the near-UV region (250–320 nm); the main chromophores in the far-UV region of the spectra are the peptide bond and the aryl ring on the side chain. Moreover, the spectra in this region respond to the CD of peptide bonds. Secondary structural variations between JCP and JCP-Ca were thus examined using CD analysis. Natural triple-helical collagen typically exhibits low positive peaks at 213–230 nm and strong negative peaks at 196–204 nm in the CD spectrum. The distinctive peak and structure of the spectrum are altered when collagen is denatured, and the positive peak at approximately 220 nm is eliminated with full denaturation (Ata et al., 2023). Moreover, full denaturation has been shown to cause the negative band to red-shift and the positive peak to completely disappear. From Fig. 1D, it can be observed that the spectra of JCP changed before and after chelating calcium ions, with a negative peak near 198 nm for JCP and a negative peak near 200 nm in the far-UV

region for each component of JCP-Ca after binding calcium ions; this was the same trend as that observed in studies by Yang et al. (2021) and Zhang, Li, Hou, Zhang, and Li (2019), which mainly manifested as the superimposed absorption of β-folding and irregular curling. Compared to those with JCP, the negative peaks of the four components of JCP-Ca at 200 nm were enhanced and red-shifted after chelation, indicating an increase in β-folding and a decrease in the content of irregular curls, which was more obvious for JCP3-Ca (Zhang et al., 2019). Generally, the negative peak at 200 nm was enhanced to a certain extent, probably due to the chelation process, and there were new ionic and covalent bonds, resulting in variation in the secondary structure of JCP-Ca from the original, disordered structure to a more ordered and regular structure, which is reflected by the position of the peak in the CD spectrum and the change in absorption intensity (Yu & Fan, 2012). Lin et al. studied tilapia (*Oreochromis niloticus*) skin iron-chelating peptides and showed that peptide folding and the creation of a more compact secondary structure were induced by iron chelation (Lin et al., 2021), consistent with our findings. This demonstrates that chelation changes the secondary structure of JCP, causing the chelate to shift towards a more ordered and regular structure.

3.4. UV spectroscopy

Variations in the intensity of the UV absorption spectra can reveal variations between calcium chelates and peptides (Wang et al., 2017). The UV spectra of JCP and its component chelates differed significantly, as illustrated in Fig. 1E. The spectra of collagen peptides showed a major absorption peak near 210 nm, which typically corresponds to specific carbonyl, carboxyl, and amide bonds in the peptides (Wu et al., 2019). In contrast to that with the collagen peptides, after calcium chelation, multiple absorption peaks in the 190–280 nm range were observed in the absorption spectra of JCP-Ca. The peptide bond C═O transition caused a notable increase in the strength of the absorption bands, as well as the red-shifting of the bands, which was clearly visible with the JCP calcium chelate. Chelation of the N and O atoms of the peptide with calcium caused a red-shift of the highest absorption peak to 227 nm, which in turn affected the peptide bond C═O transition. In addition, the increase in absorbance with an increasing molecular weight could be due to the bonding of the intermediate ions of the chelate with the ligand, leading to internal electron transition within the ligand, which requires different energy than that required for the internal electron transition within the free ligand. The UV absorption of the calcium chelate varies concurrently with the valence electrons of the relevant atoms. Following chelation, the strength of the absorption peaks increased and a color-enhancing effect was observed. In a complex of human-like collagen with calcium (Yu & Fan, 2012), there have also been reports of an increase in the uptake intensity and a red-shift in the maximal uptake. These findings imply that the spatial structure is altered with the peptides of chromophores and auxiliary pigments upon binding to calcium ions. Zhao et al. (2014) studied whey protein hydrolysate–calcium chelates and found that light absorption intensity was enhanced upon binding to calcium, which agrees with our results. Therefore, it can be concluded that a chelation reaction occurs between collagen peptides and calcium ions.

3.5. Fluorescence spectroscopy

Among protein molecules, aromatic amino acids hold a distinct position due to their unique structural feature of containing a benzene ring. These include tryptophan (Trp), tyrosine (Tyr), and phenylalanine (Phe). In particular, the microenvironment around tryptophan residues is polar; they fluoresce and produce emission spectra because of variations in the side-chain chromophores and the uniqueness of their chemical structures. Thus, variations in the strength and wavelength of the fluorescence spectrum can be used to identify structural alterations between amino acid groups and mineral ions (Lin et al., 2020). From the fluorescence results shown in Fig. 1F, the maximum absorption peak of the collagen peptides and chelates of each isolated component was observed at 350 nm. Based on the proximity between the two residues, the energy transfer from Tyr to Trp and the quenching group on nearby amino acid residues had the greatest effect on the fluorescence intensity. The fluorescence intensity occurred in the order JCP4-Ca > JCP3-Ca > JCP2-Ca > JCP1-Ca and was markedly different in each. This increase could have resulted from intricate interactions between calcium and the chromophore that modifies the energy of the excited state, which in turn influences the intensity. This fraction had a distinct fluorescence intensity because it was separated using an ultrafiltration tube with a different molecular weight, which would also affect the polypeptide chain length and separation between the Tyr and Trp residues in each portion (Shao, Wang, Zhang, Zhang, & Hao, 2022). Sun et al. (2020) found that when herring egg phosphopeptides were bound to calcium, the intensity of the endogenous fluorescence increased, consistent with our findings. The binding of jellyfish collagen peptides to calcium ions caused structural alterations in the peptides and amino acids, leading to folding and aggregation, suggesting that JCP binding was successful for calcium ions, a new substance was produced, and the fluorescence intensity of its chelate increased with an increasing molecular weight.

3.6. Analysis of 3D fluorescence spectra

Excitation–emission matrix fluorescence spectroscopy, a type of 3D fluorescence spectroscopy, is useful for examining intricate conformational changes in proteins. It can accurately display the fluorescence data of a sample, thereby enhancing its scientific validity and credibility. The 3D fluorescence spectra of JCP and JCP-Ca are shown in Fig. 2, with a peak representing the intrinsic fluorescence properties of JCP due to the $\pi \rightarrow \pi^*$ transitions involved in the Trp and Tyr residues, reflecting the change in the tertiary structure of JCP after complexation with calcium ions (Feroz, Mohamad, Bujang, Malek, & Tayyab, 2012). Peak *a* of JCP was substantially reduced upon binding to calcium ions, which can be attributed to the generation of a stabilizing ground-state complex in JCP-Ca, which would decrease the fluorescence emission from Trp and Tyr residues in JCP. In addition, JCP-Ca showed an overall red-shift from the position of JCP peak *a*. This could be because chelation with calcium ions exposes the aromatic amino acids within the protein, which increases the polarity of the environment in which the chromophore group is located. In contrast, peak *b* was associated with the fluorescence characteristics of the major structure of the JCP polypeptide induced by the $n \rightarrow \pi^*$ transition, reflecting the changes in these secondary structures of JCP in the presence of calcium ions (Zaroog & Tayyab, 2012). The emission wavelength of peak *c*, which was a first-order Rayleigh scattering peak, was equal to the excitation wavelength. Because JCP binds to calcium ions, there is an increased possibility of light scattering, which accounted for the increase in peak *c* of JCP compared to that of the four JCP-Ca samples. Changes in peaks *a*, *b*, and *c* in the 3D fluorescence spectra indicated unfolding of the polypeptide chains, leading to conformational changes and the binding of JCP to calcium ions, resulting in stable complexes.

3.7. SEM

SEM is a sophisticated and up-to-date analytical method in which small or undetectable materials are magnified thousands of times. As such, SEM has a resolution of several nanometers. Consequently, SEM is typically used for morphological observations and quantitative elemental composition analyses. Fig. 3 shows the SEM images of JCP and different fractions of JCP-Ca, magnified 500 and 2000 times. JCP was found to have a smooth surface with an irregular crystal-like shape. In contrast to JCP, JCP-Ca featured a rough surface with a granular structure and a dense size distribution. This could be because metal ions can interact with peptides and substantially affect their aggregation (Sharma, Pavlova, Kim, Kim, & Mirica, 2013). The different fractions of

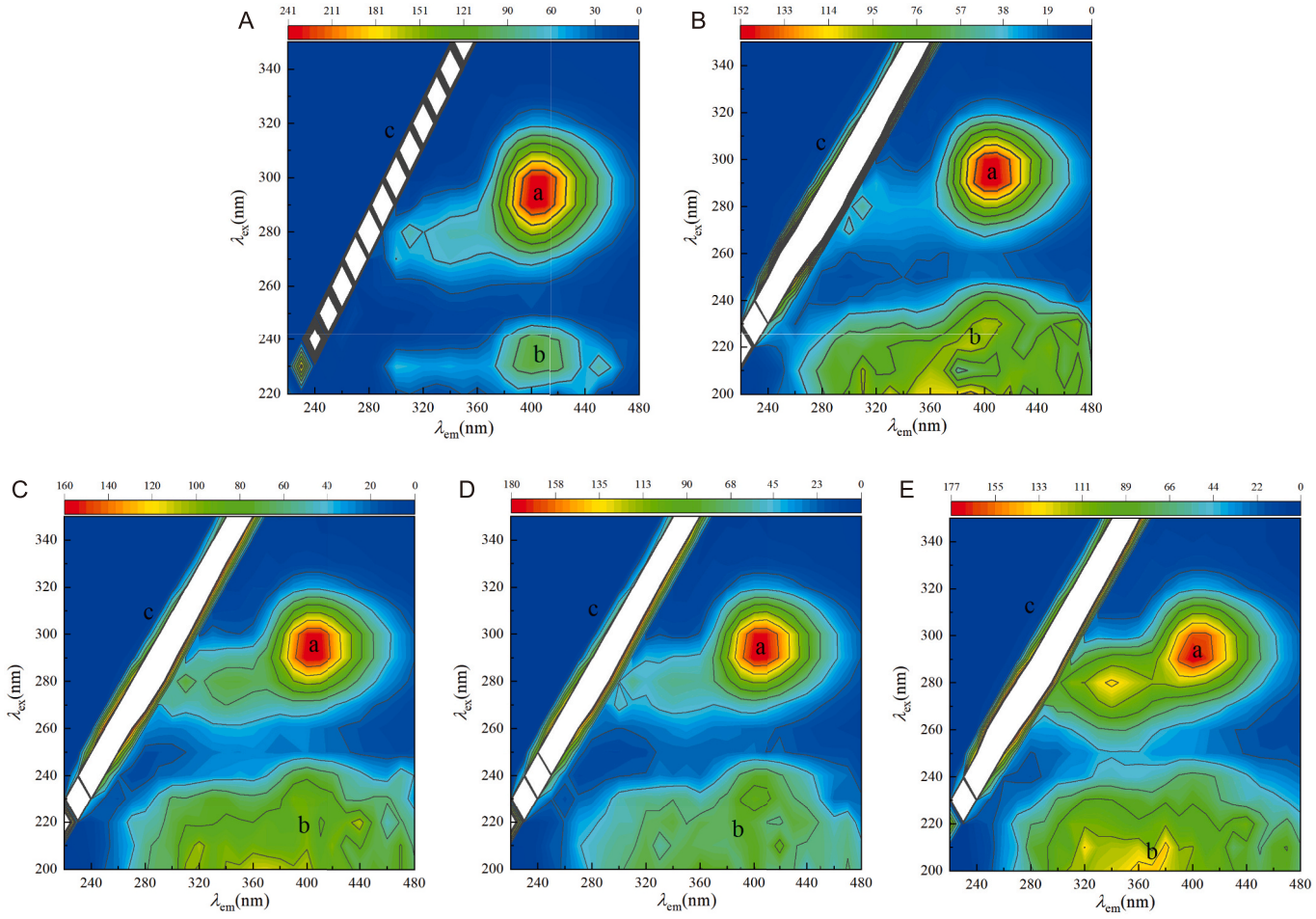

Fig. 2. Three-dimensional (3D) fluorescence spectra of jellyfish collagen peptide (JCP) and different fractions of JCP–calcium chelates (JCP-Ca): JCP (A), JCP1-Ca (B), JCP2-Ca (C), JCP3-Ca (D), and JCP4-Ca (E).

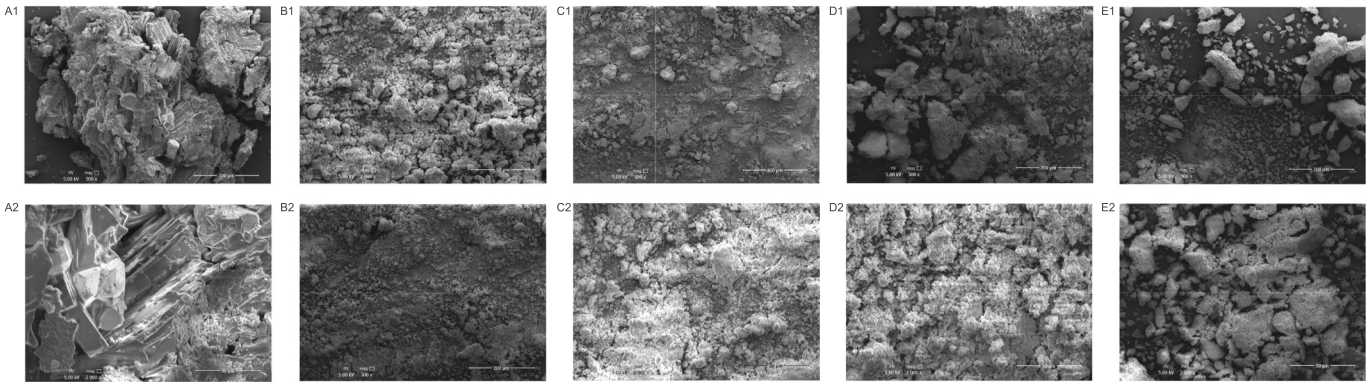

Fig. 3. Scanning electron microscopy (SEM) microstructures of jellyfish collagen peptide (JCP) and JCP–calcium complex (JCP-Ca) components with different molecular weights. (A) SEM microstructures of JCP at 500× (A1) and 2000× (A2); (B) SEM microstructures of JCP1-Ca^{2+} at 500× (B1) and 2000× (B2); (C) SEM microstructures of JCP2-Ca^{2+} at 500× (C1) and 2000× (C2); (D) SEM microstructures of JCP3-Ca^{2+} at 500× (D1) and 2000× (D2); (E) SEM microstructures of JCP4-Ca^{2+} at 500× (E1) and 2000× (E2).

JCP-Ca are presented in Fig. 3A–E; Fig. 3E shows that JCP4-Ca had a relatively loose structure compared to the other three fractions; small-molecular-weight peptides are more likely to combine during ultrafiltration and produce a denser structure, which could be the source of this difference (Shao et al., 2022). Moreover, JCP1-Ca (Fig. 3B) and JCP3-Ca (Fig. 3D) had a denser distribution of granular structures, probably because of the higher chelation rate of JCP1 and JCP3 and the higher calcium ion contents. Morphological analyses of small-molecular-weight peptides indicated that they were more likely to form denser structures.

3.8. Determination of antioxidant capacity

3.8.1. Fe^{3+} reducing power

Antioxidant capacity is mostly represented by the electron or

hydrogen supply, and the measured antioxidant capacity is primarily obtained by determining the reducing power. As shown in Fig. 4A, the reducing power of JCP and each component of the JCP-Ca chelate increased linearly with an increasing mass concentration. The four components, the reducing power of JCP3-Ca was remarkably higher than that of the other components; the maximum absorbance reached 0.114 at a dose of 5 mg/mL, indicating that it had more reducing power than the other components. By comparison, the reducing power of JCP was not as strong as that of each component of JCP-Ca; the reason for this could be that chelates contain more amino acid residues and that these amino acid residues are generally reducing in nature. Chelation with metal ions has been shown to result in comparable outcomes in several prior trials. According to Fang et al. (2020), Manchurian walnut protein hydrolysates and Manchurian walnut protein hydrolysates–calcium show lower scavenging abilities against DPPH and ABTS radicals, respectively. In addition, MWPH–Ca demonstrated greater antioxidant activity than MWPH, which was consistent with our findings. Moreover, peptide Fe^{3+} reduction was greatly enhanced by calcium ion chelation, and JCP3-Ca exhibited greater reducing capability.

3.8.2. *DPPH radical-scavenging activity*

Because DPPH is a persistent free radical that reaches its maximum absorbance in methanol at 517 nm, it is frequently used to assess reducing chemicals, particularly natural compounds (Jamdar, Rajalakshmi, & Sharma, 2012). For DPPH radicals, for which the methanol solution is purple in color, an antioxidant will result in purple color fading; therefore, the change in absorbance can be used to determine the antioxidant capacity of the sample. Both the peptide and its calcium chelate exhibited concentration-dependent antioxidant activities. As shown in Fig. 4B, both JCP and different fractions of JCP-Ca showed a trend of higher DPPH radical-scavenging with an increase in the mass concentration. At the same concentration, the antioxidant activity of the chelates was greater than that of the active peptides, indicating that chelation enhanced the antioxidant activity of the peptides. This is probably because the chelation reaction of metal ions with specific groups in each component of JCP increases the hydrophobic amino acids in the reaction system, thereby increasing the antioxidant activity of the peptide–calcium chelates (Yang, Lian, Duan, Ma, & Zhang, 2023). Onuh, Girgih, Aluko, and Aliani (2014) found that the peptide fractions of

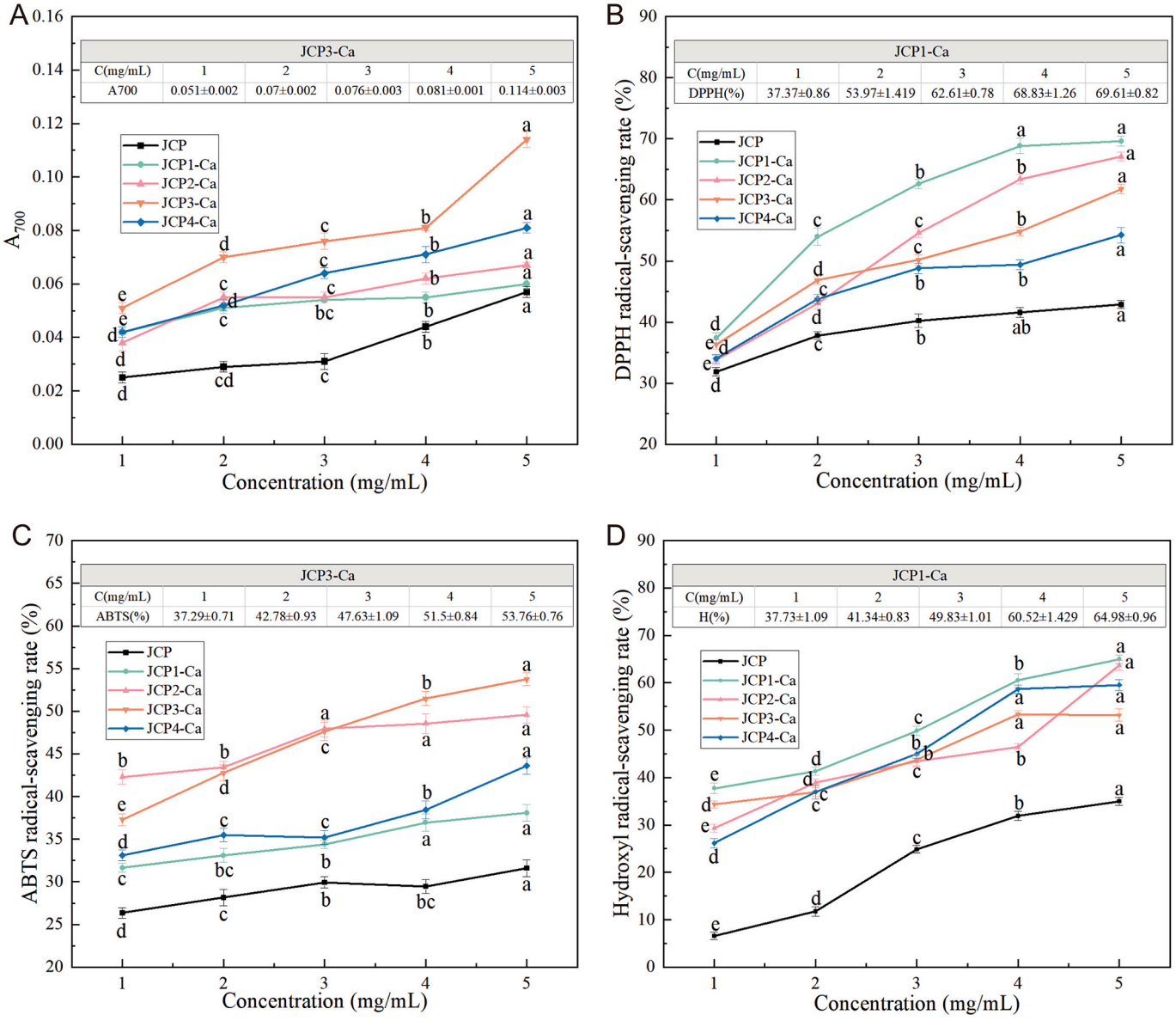

Fig. 4. Antioxidant activity of jellyfish collagen peptide–calcium complex (JCP-Ca). (A) Fe^{3+} reducing power; (B) DPPH radical-scavenging activity; (C) ABTS radical-scavenging activity; (D) hydroxyl radical-scavenging activity.

chicken skin proteolytic digests with molecular weights <1 kDa showed the highest DPPH radical-scavenging capacity, which is consistent with our results. The overall trend in the DPPH radical-scavenging ability of each component was JCP1-Ca > JCP2-Ca > JCP3-Ca > JCP4-Ca > JCP, in descending order. These findings suggest that peptides with lower molecular weights that are chelated with calcium would be more effective at scavenging DPPH radicals and that the antioxidant activity of the chelates would be greater than that of the active peptides.

3.8.3. ABTS radical-scavenging activity

The Trolox-equivalent antioxidant capacity, which represents the ABTS radical-scavenging ability, is used to quantify the antioxidant activity of a substance in relation to the Trolox standard (Samaranayaka & Li-Chan, 2011). The ABTS radical-scavenging capacities of JCP and JCP-Ca are shown in Fig. 4C. The capacity of each sample to scavenge ABTS radicals was positively correlated with its concentration. The overall trend indicated a more rapid increase in ABTS radical-scavenging capacity for JCP3-Ca and a more moderate increase for the other groups, with JCP3-Ca showing better ABTS radical-scavenging capacity. Alashi et al. (2014) found strong ABTS radical-scavenging ability in rapeseed enzymatic digests, with the <1 kDa peptide fractions having the best activity, where Ngoh and Gan (2016) found that the <3 kDa peptide fractions in zebu bean enzymatic digests had the highest ABTS radical-scavenging ability, which contrasted with our results. This implies that the amino acid composition and sequence, as well as the corresponding molecular mass, affect the antioxidant activity of collagen peptides. At the same concentration, JCP3-Ca had better reducing ability and the chelate exhibited a higher level of antioxidant activity than the active peptide, indicating that the ability of each JCP component to scavenge ABTS is improved following chelation.

3.8.4. Determination of hydroxyl radical-scavenging activity

Hydroxyl radicals, which are produced by the Fenton reaction when H_2O_2 reacts with metal ions, such as Fe (II) or Cu (II), are highly-reactive transient species that can hydroxylate DNA, proteins, and lipids. Additionally, they can combine with aromatic chemicals to produce hydroxyl cyclohexadienyl radicals, which can then be broken down into phenoxy radicals or peroxyl radicals after reacting with oxygen (Jamdar et al., 2012). The magnitudes of the hydroxyl radical-scavenging capacity of JCP and the JCP-Ca of different molecular weights are shown Fig. 4D: This figure illustrates that as the peptide content is increased, the ability of each group to scavenge hydroxyl radicals is increased. Hydroxyl

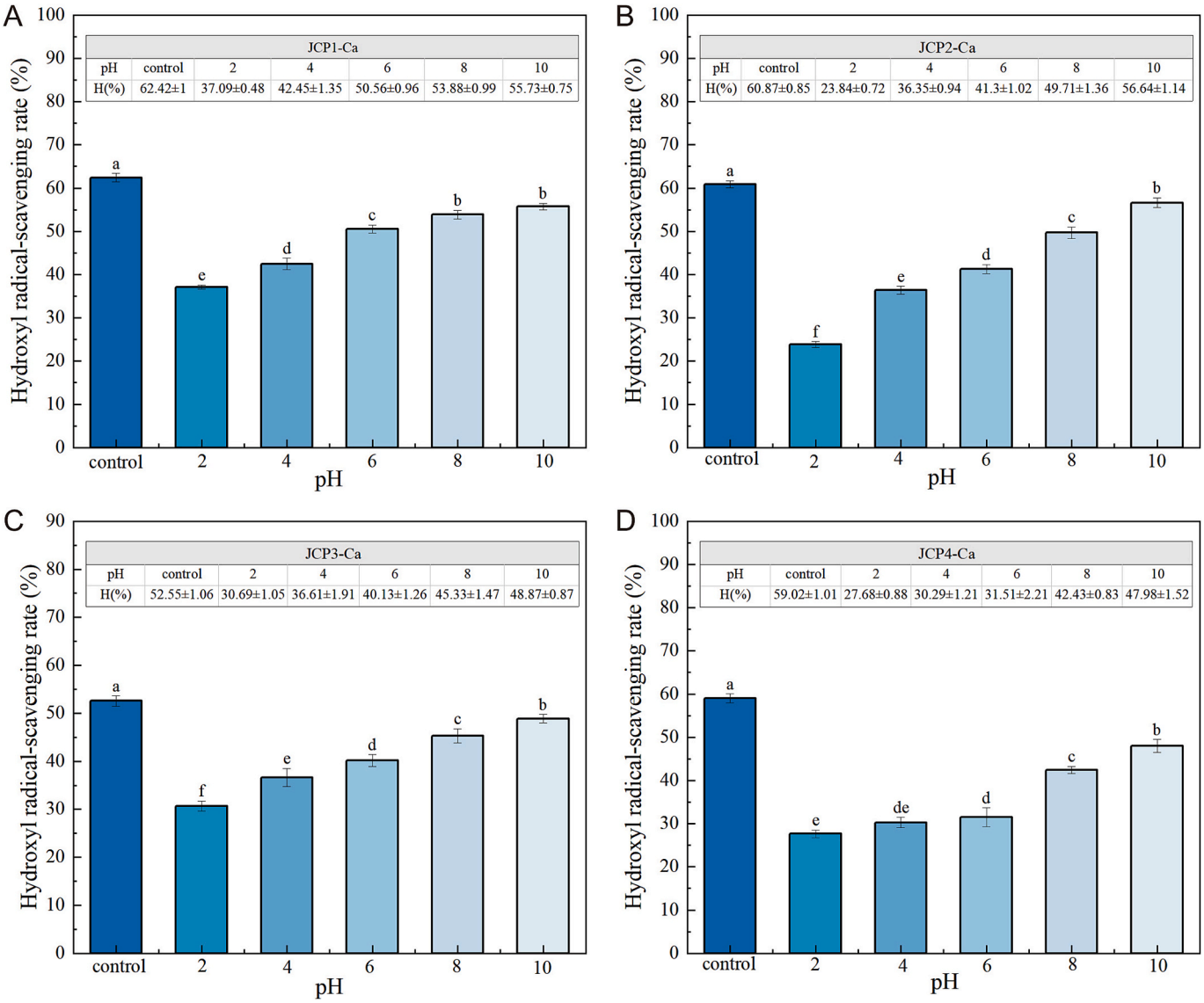

Fig. 5. Stability of different fractions of the jellyfish collagen peptide–calcium complex (JCP-Ca) under different pH conditions. (A) Stability of JCP1-Ca; (B) stability of JCP2-Ca; (C) stability of JCP3-Ca; (D) stability of JCP4-Ca.

radicals can be destructive to cells in an organism mainly because these free radicals commonly react with substances in the cells, thereby altering these substances and changing the cells. The hydroxyl radical-scavenging ability of JCP1-Ca with a molecular weight of <1 kDa was noticeably higher than that of the other molecular weight fractions when the concentrations of the sample solutions were the same, and this reached a maximum at a concentration of 5 mg/mL, with a hydroxyl radical-scavenging ability of up to 64.98 ± 0.66%. Jamdar et al. (2012)

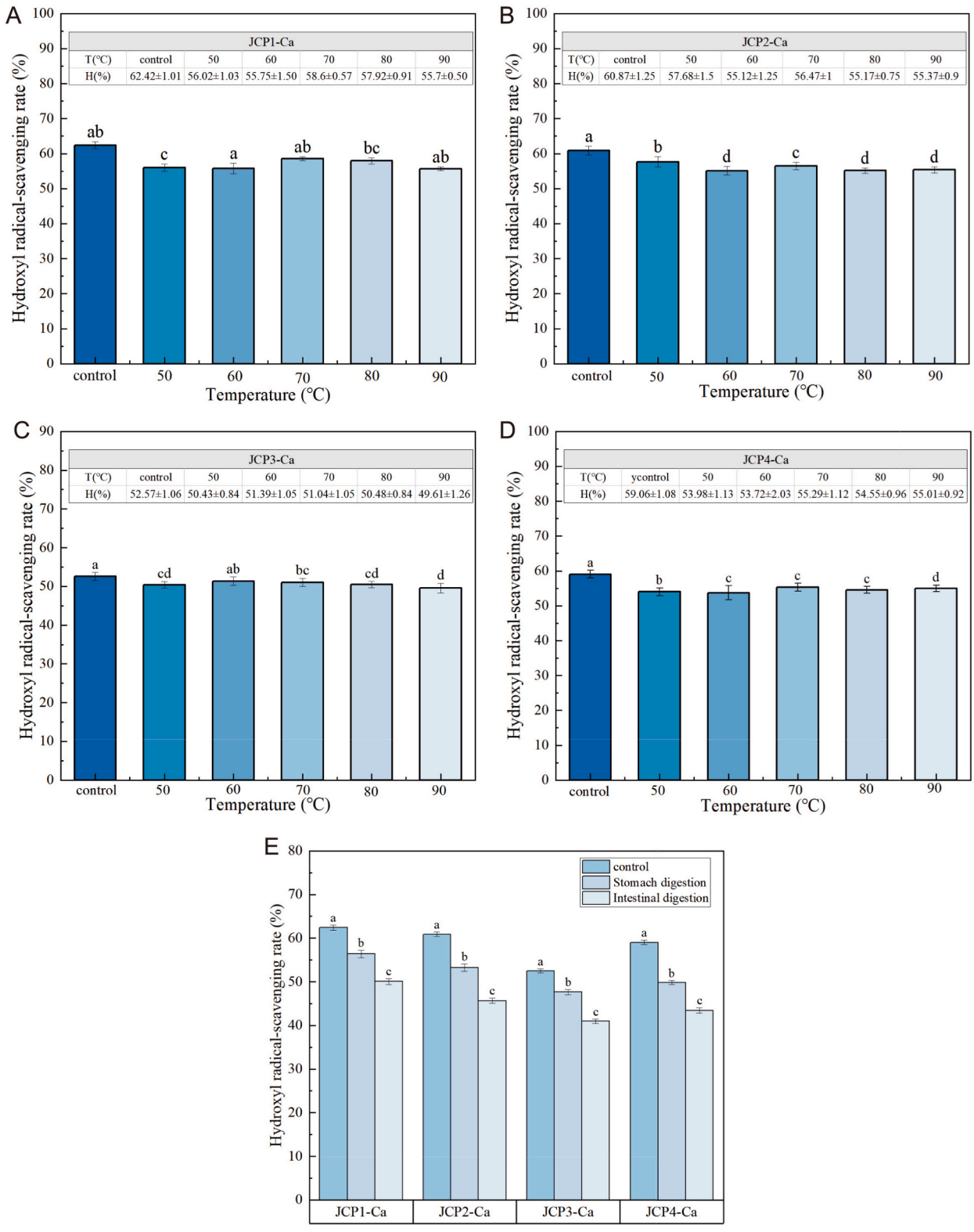

Fig. 6. Stability of different components of the jellyfish collagen peptide–calcium complex (JCP-Ca) under different temperature conditions. (A) Stability of JCP1-Ca; (B) stability of JCP2-Ca; (C) stability of JCP3-Ca; (D) stability of JCP4-Ca; (E) stability of different fractions of jellyfish collagen peptide–calcium complex (JCP-Ca) during in vitro simulated gastrointestinal digestion.

found that small peptides (<3 kDa) of different fractions of poultry visceral protein hydrolysates had a better capacity for scavenging hydroxyl radicals. However, the hydroxyl radical-scavenging capacities of the four fractions at each concentration did not differ statistically. In comparison, it is evident that the radical-scavenging capacity of JCP was not as good as that of the JCP-Ca components. In conclusion, the hydroxyl radical-scavenging ability of low-molecular-weight peptide chelates surpasses that of high-molecular-weight peptide chelates.

3.9. Analysis of JCP-ca stability

3.9.1. pH and temperature

Fig. 5 shows the stability of JCP-Ca at various pH values. Following various pH treatments, the ability of the peptide–calcium chelate to scavenge free radicals declined compared to that of the control. These findings imply that at low pH levels, peptide–calcium chelates that can scavenge free radicals could lose some of their activity. This could be because high H^+ concentrations compete with Ca^{2+} and capture the peptide sites that are attached to Ca^{2+}, causing the disintegration and release of calcium ions from JCP-Ca (Luo, Yao, Soladoye, Zhang, & Fu, 2022), which results in a decrease in hydroxyl radical-scavenging activity. JCP-Ca was stable in alkaline environments.

The temperature stability is shown in Fig. 6. In the range of 50–90 °C, the ability of the component peptide–calcium chelate to scavenge free radicals was marginally reduced when the temperature was increased relative to that of the control, but this decrease was not significant, indicating that the chelates were resistant to thermal processing. To summarize the results, the antioxidant activity of JCP-Ca was relatively stable at temperatures of 50–90 °C; however, the antioxidant activity decreased under strong acid conditions ($p < 0.05$). As such, heat treatment can be applied during the processing and storage of its related products, but the effects of strong acid conditions should be avoided.

3.9.2. In vitro simulated digestion

Dietary nutrients are generally absorbed by the gut via gastric digestion, peptides can be degraded by pepsin and trypsin enzymes to form smaller molecules or amino acids, respectively; and peptide bioactivities can be adversely modified. One method to assess the digestive stability of bioactive compounds is to determine their resistance to trypsin and pepsin. Fig. 6E illustrates how the peptide–calcium chelates could scavenge hydroxyl radicals in the gastrointestinal tract. Following simulated gastric fluid digestion, the hydroxyl radical-scavenging rates of all JCP-Ca fractions decreased. These findings indicate that pepsin is sensitive to pH and has a minor effect on the stability of the chelates, which leads to the dissociation of bound calcium into its ionic state. Small-molecular-weight peptides are less susceptible to pepsin hydrolysis, according to research by Wu and Ding (2002). The hydroxyl radical-scavenging rates of the fractions decreased to 50.3 ± 0.7%, 43.66 ± 0.65%, 40.98 ± 0.51%, and 43.45 ± 0.6%, respectively, following further treatment with simulated intestinal fluids. The acidic environment of the stomach can cause structural alterations to peptides, thereby reducing their capacity to bind calcium ions. Moreover, trypsin might have caused the peptide to break down, which would have decreased its ability to bind calcium ions (Wu et al., 2019), further leading to a decrease in the rate of hydroxyl radical-scavenging; however, its antioxidant activity was still maintained at >71% of its original activity. Better digestive stability of a compound favors its use as a functional ingredient in related products, which is favorable for its application as a functional raw material for related products.

However, this study solely investigated the structural properties and biological activities of calcium and peptide chelates, without delving into the precise mechanism by which peptide calcium chelates enhance calcium absorption. Therefore, further research is warranted in this regard.

4. Conclusion

JCP was used as a matrix to construct collagen peptide–calcium chelates through binding to calcium ions. Spectroscopic and scanning electron microscopic analyses showed that JCP can form stable chelates with calcium ions; moreover, the spectral properties of chelates formed by JCP of different molecular weights and calcium ions differed, and the intensity increased with an increase in the molecular weight. An analysis of antioxidant activity further demonstrated that the binding of JCP to calcium ions enhanced its antioxidant activity, with JCP1-Ca having better DPPH- and hydroxyl radical-scavenging activity and JCP3-Ca having better ABTS radical-scavenging activity and reducing power. The stability analysis indicates that the prepared JCP-Ca exhibits relative stability across various temperatures, rendering it suitable for hot processing; however, its compatibility with acidic products is not low. Moreover, JCP-Ca was found to have high stability under simulated gastrointestinal digestion conditions. In conclusion, the present study demonstrates the feasibility of preparing peptide–calcium chelates using jellyfish and provides a reasonable basis for the application of JCP-Ca as an active antioxidant or jellyfish dietary supplement application prospects.

CRediT authorship contribution statement

Jiajia Gao: Writing – original draft, Validation, Methodology, Conceptualization. **Chong Ning:** Validation, Software, Methodology, Data curation. **Mingming Wei:** Software, Data curation, Conceptualization. **Yifei Ren:** Software. **Weixuan Li:** Writing – review & editing, Supervision, Resources, Project administration, Methodology, Conceptualization.

Declaration of competing interest

We wish to draw the attention of the Editor to the following facts which may be considered as potential conflicts of interest and to significant financial contributions to this work.

We wish to confirm that there are no know conflicts of interest associated with this publication and there has been no significant financial support for this work that could have influenced its outcome.

We confirm that the manuscript has been read and approved by all named authors and that there is no other person who satisfied the criteria for authorship but are not listed. We further confirm that the order of authors listed in the manuscript has been approved by all of us.

We confirm that we have given due consideration to the protection of intellectual property associated with this work and that there are no impediments to publication, including the timing of publication, with respect to intellectual property. In so doing we confirm that we have followed the regulations of our institutions concerning intellectual property.

We understand that the Corresponding Author is the sole contact for the Editorial process (including Editorial Manager and direct communications with the office). He/she is responsible for communicating with the other authors about progress, submissions of revisions and final approval of proofs. We confirm that we have provided a current, correct email address which is accessible by the Corresponding Author and which has been configured to accept email from (liweixuan@lnu.edu.cn) signed by all authors as follows:

Data availability

Data will be made available on request.

Acknowledgment

This work was supported by Yingkou City Enterprise Doctor double innovation plan project: jellyfish production “stuck neck” problem and

high value utilization of processing materials. We would like to thank Editage (www.editage.cn) for English language editing.

References

Alashi, A. M., Blanchard, C. L., Mailer, R. J., Agboola, S. O., Mawson, A. J., He, R., et al. (2014). Antioxidant properties of Australian canola meal protein hydrolysates. *Food Chemistry, 146*, 500–506.

Ata, O., Bakar, B., Turkoz, B. K., Kumcuoglu, S., Aydogdu, Y., Gumustas, B., et al. (2023). Structural and molecular characterization of collagen-type I extracted from lamb feet. *Journal of Food Science*, 1–12.

Chen, M., Chen, C., Zhang, Y., Jiang, H., Fang, Y., & Huang, G. (2023). Effects of iron-peptides chelate nanoliposomes on iron supplementation in rats. *Biological Trace Element Research, 201*, 4508–4517.

Choi, D. W., Lee, J. H., Chun, H. H., & Song, K. B. (2012). Isolation of a calcium-binding peptide from bovine serum protein hydrolysates. *Food Science and Biotechnology, 21*, 1663–1667.

Fan, J., Zhuang, Y., & Li, B. (2013). Effects of collagen and collagen hydrolysate from jellyfish umbrella on histological and immunity changes of mice photoaging. *Nutrients, 5*, 223–233.

Fang, S., Ruan, G., Hao, J., Regenstein, J. M., & Wang, F. (2020). Characterization and antioxidant properties of manchurian walnut meal hydrolysates after calcium chelation. *LWT - Food Science and Technology, 130*, Article 109632.

Feroz, S. R., Mohamad, S. B., Bujang, N., Malek, S. N., & Tayyab, S. (2012). Multispectroscopic and molecular modeling approach to investigate the interaction of flavokawain B with human serum albumin. *Journal of Agricultural and Food Chemistry, 60*, 5899–5908.

Ge, M. X., Chen, R. P., Zhang, L., Wang, Y. M., Chi, C. F., & Wang, B. (2023). Novel ca-chelating peptides from protein hydrolysate of Antarctic krill (Euphausia superba): Preparation, characterization, and calcium absorption efficiency in Caco-2 cell monolayer model. *Marine Drugs, 21*(11).

Hu, Y. D., Xi, Q. H., Kong, J., Zhao, Y. Q., Chi, C. F., & Wang, B. (2023). Angiotensin-I-converting enzyme (ACE)-inhibitory peptides from the collagens of monkfish (Lophius litulon) swim bladders: Isolation, characterization, molecular docking analysis and activity evaluation. *Marine Drugs, 21*(10).

Huang, G., Ren, L., & Jiang, J. (2010). Purification of a histidine-containing peptide with calcium binding activity from shrimp processing byproducts hydrolysate. *European Food Research and Technology, 232*, 281–287.

Huang, W., Lan, Y., Liao, W., Lin, L., Liu, G., Xu, H., et al. (2021). Preparation, characterization and biological activities of egg white peptides-calcium chelate. *LWT - Food Science and Technology, 149*, Article 112035.

Jamdar, S. N., Rajalakshmi, V., & Sharma, A. (2012). Antioxidant and ace inhibitory properties of poultry viscera protein hydrolysate and its peptide fractions. *Journal of Food Biochemistry, 36*, 494–501.

Li, C., Bu, G., Chen, F., & Li, T. (2020). Preparation and structural characterization of peanut peptide–zinc chelate. *CyTA Journal of Food, 18*, 409–416.

Lin, S., Hu, X., Li, L., Yang, X., Chen, S., Wu, Y., et al. (2021). Preparation, purification and identification of iron-chelating peptides derived from tilapia (*Oreochromis niloticus*) skin collagen and characterization of the peptide-iron complexes. *LWT - Food Science and Technology, 149*, Article 111796.

Lin, Y., Cai, X., Wu, X., Lin, S., & Wang, S. (2020). Fabrication of snapper fish scales protein hydrolysate-calcium complex and the promotion in calcium cellular uptake. *Journal of Functional Foods, 65*, Article 103717.

Luo, J., Yao, X., Soladoye, O. P., Zhang, Y., & Fu, Y. (2022). Phosphorylation modification of collagen peptides from fish bone enhances their calcium-chelating and antioxidant activity. *LWT - Food Science and Technology, 155*, Article 112978.

Lv, Z., Zhang, C., Song, W., Chen, Q., & Wang, Y. (2022). Jellyfish Collagen Hydrolysate Alleviates Inflammation and Oxidative Stress and Improves Gut Microbe Composition in High-Fat Diet-Fed Mice. *Mediators of Inflammation, 8*, 5628702.

Ngoh, Y. Y., & Gan, C. Y. (2016). Enzyme-assisted extraction and identification of antioxidative and α-amylase inhibitory peptides from pinto beans (*Phaseolus vulgaris* cv. Pinto). *Food Chemistry, 190*, 331–337.

Onuh, J. O., Girgih, A. T., Aluko, R. E., & Aliani, M. (2014). In vitro antioxidant properties of chicken skin enzymatic protein hydrolysates and membrane fractions. *Food Chemistry, 150*, 366–373.

Peng, Z., Hou, H., Zhang, K., & Li, B. (2017). Effect of calcium-binding peptide from Pacific cod (*Gadus macrocephalus*) bone on calcium bioavailability in rats. *Food Chemistry, 221*, 373–378.

Samaranayaka, A. G. P., & Li-Chan, E. C. Y. (2011). Food-derived peptidic antioxidants: A review of their production, assessment, and potential applications. *Journal of Functional Foods, 3*, 229–254.

Shao, J., Wang, M., Zhang, G., Zhang, B., & Hao, Z. (2022). Preparation and characterization of sesame peptide-calcium chelate with different molecular weight. *International Journal of Food Properties, 25*, 2198–2210.

Sharma, A. K., Pavlova, S. T., Kim, J., Kim, J., & Mirica, L. M. (2013). The effect of Cu^{2+} and Zn^{2+} on the $A\beta_{42}$ peptide aggregation and cellular toxicity. *Metallomics, 5*, 1529–1536.

Sun, N., Wang, Y., Bao, Z., Cui, P., Wang, S., & Lin, S. (2020). Calcium binding to herring egg phosphopeptides: Binding characteristics, conformational structure and intermolecular forces. *Food Chemistry, 310*, Article 125867.

Sun, R., Liu, X., Yu, Y., Miao, J., Leng, K., & Gao, H. (2021). Preparation process optimization, structural characterization and *in vitro* digestion stability analysis of Antarctic krill (*Euphausia superba*) peptides-zinc chelate. *Food Chemistry, 340*, Article 128056.

Wali, A., Wubulikasimu, A., Yanhua, G., Omar, A., Arken, A., Yili, A., & Aisa, H. A. (2019). Separation and purification of antioxidant peptides from enzymatically prepared scorpion (Buthus martensii Karsch) protein hydrolysates. *International Journal of Peptide Research and Therapeutics, 26*(4), 1803–1818.

Wang, X., Gao, A., Chen, Y., Zhang, X., Li, S., & Chen, Y. (2017). Preparation of cucumber seed peptide-calcium chelate by liquid state fermentation and its characterization. *Food Chemistry, 229*, 487–494.

Wang, Y., Cai, M., Zeng, H., Zhao, H., Zhang, M., & Yang, Z. (2022). Preparation, characterization and iron absorption by Caco-2 cells of the casein peptides-iron chelate. *International Journal of Peptide Research and Therapeutics, 28*, 116.

Wang, Y.-Y., Wang, C.-Y., Wang, S.-T., Li, Y.-Q., Mo, H.-Z., & He, J.-X. (2021). Physicochemical properties and antioxidant activities of tree peony (Paeonia suffruticosa Andr.) seed protein hydrolysates obtained with different proteases. *Food Chemistry, 345*.

Wu, J., & Ding, X. (2002). Characterization of inhibition and stability of soy-protein-derived angiotensin I-converting enzyme inhibitory peptides. *Food Research International, 35*, 367–375.

Wu, W., He, L., Liang, Y., Yue, L., Peng, W., Jin, G., et al. (2019). Preparation process optimization of pig bone collagen peptide-calcium chelate using response surface methodology and its structural characterization and stability analysis. *Food Chemistry, 284*, 80–89.

Wu, Y., Chen, S., Luo, P., Deng, S., Shan, Z., Fang, J., et al. (2022). Optimizing the biodegradability and biocompatibility of a biogenic collagen membrane through cross-linking and zinc-doped hydroxyapatite. *Acta Biomaterialia, 143*, 159–172.

Xiang, H., Huang, H., Sun, W. D., Hu, X., Li, L., Waterhouse, G., et al. (2022). Enzymatically synthesized γ-$[Glu]_{(n\geq1)}$-Gln as novel calcium-binding peptides to deliver calcium with enhanced bioavailability. *Food Chemistry, 387*, Article 132918.

Yang, J., Lian, H., Duan, Y., Ma, H., & Zhang, H. (2023). Preparation and bioavailability of *Chlorella pyrenoidosa* protein hydrolysates-calcium chelate. *Algal Research, 75*, Article 103263.

Yang, J., Shao, J., Duan, Y., Geng, F., Jin, W., Zhang, H., … Deng, Q. (2024). Insights into digestibility, biological activity, and peptide profiling of flaxseed protein isolates treated by ultrasound coupled with alkali cycling. *Food Research International, 190*, 114629.

Yang, X., Yu, X., Yagoub, A. G., Chen, L., Wahia, H., Osae, R., et al. (2021). Structure and stability of low molecular weight collagen peptide (prepared from white carp skin) -calcium complex. *LWT - Food Science and Technology, 136*, Article 110335.

Yu, H., Li, R., Liu, S., Xing, R., Chen, X., & Li, P. (2014). Amino acid composition and nutritional quality of gonad from jellyfish *Rhopilema esculentum*. *Biomedicine & Preventive Nutrition, 4*, 399–402.

Yu, Y., & Fan, D. (2012). Characterization of the complex of human-like collagen with calcium. *Biological Trace Element Research, 145*, 33–38.

Zamorano-Apodaca, J. C., Garcia-Sifuentes, C. O., Carvajal-Millan, E., Vallejo-Galland, B., Scheuren-Acevedo, S. M., & Lugo-Sanchez, M. E. (2020). Biological and functional properties of peptide fractions obtained from collagen hydrolysate derived from mixed by-products of different fish species. *Food Chemistry, 331*, Article 127350.

Zaroog, M. S., & Tayyab, S. (2012). Formation of molten globule-like state during acid denaturation of *aspergillus Niger* glucoamylase. *Process Biochemistry, 47*, 775–784.

Zhang, K., Li, J., Hou, H., Zhang, H., & Li, B. (2019). Purification and characterization of a novel calcium-biding decapeptide from Pacific cod (*Gadus Macrocephalus*) bone: Molecular properties and calcium chelating modes. *Journal of Functional Foods, 52*, 670–679.

Zhang, M., & Liu, K. (2022). Calcium supplements and structure-activity relationship of peptide-calcium chelates: A review. *Food Science and Biotechnology, 31*, 1111–1122.

Zhang, S.-Y., Zhao, Y.-Q., Wang, Y.-M., Yang, X.-R., Chi, C.-F., & Wang, B. (2022). Gelatins and antioxidant peptides from skipjack tuna (Katsuwonus pelamis) skins: Purification, characterization, and cytoprotection on ultraviolet-A injured human skin fibroblasts. *Food Bioscience, 50*.

Zhao, L., Huang, Q., Huang, S., Lin, J., Wang, S., Huang, Y., et al. (2014). Novel peptide with a specific calcium-binding capacity from whey protein hydrolysate and the possible chelating mode. *Journal of Agricultural and Food Chemistry, 62*, 10274–10282.

Zhong, Y., Zhou, Y., Ma, M., Zhao, Y., Xiang, X., Shu, C., et al. (2023). Preparation, structural characterization, and stability of low-molecular-weight collagen peptides-calcium chelate derived from tuna bones. *Foods, 12*, 3403.